Effects of Fe-Doping on the Structural and Magnetic Properties of Indium Oxide Nanoparticles Synthesized by Bottom up Technique

M. Naeem[1], K. Kamran[1], S. Qaseem[1], S. Rizwan Ali[1,*] and S. Imran Ali[2]

[1]*Department of Physics, Federal Urdu University of Arts, Science and Technology Karachi Pakistan*

[2]*Department of Applied Chemistry and Chemical Technology, University of Karachi, Karachi, Pakistan*

Abstract: We study Fe doped In_2O_3 nanoparticles (NPs) from structural and magnetic point of view. X-ray diffraction (XRD) and transmission electron microscopy (TEM) reveal cubic bixbyite structure for both pure and Fe doped samples thereby confirming successful incorporation of Fe in host In_2O_3 lattice. Average crystallite size of pure and Fe doped (5% and 10%) In_2O_3 as calculated by Scherer's formula shows slight increase from 21 nm for pure to 27 nm for the sample with 10% Fe content. The Williamson Hall (WH) method was also utilized to further determine crystallite size and Fe induced strain in In_2O_3 lattice. The crystallite sizes by WH plot are found to be 18 nm (for undoped), 22 nm (for 5% Fe) and 24 nm (for 10% Fe). These values are in good agreement with TEM results. Energy dispersive x-ray spectroscopy (EDX) indicates the existence of some oxygen vacancies in Fe doped In_2O_3 samples. Magnetic measurements show that all Fe doped In_2O_3 NPs exhibit typical ferromagnetic hysteresis loop with saturation magnetization M_s increasing with increasing Fe concentration. Temperature dependence of field cooled (FC) and zero field cooled (ZFC) magnetizations show no divergence and transition from ferromagnetism to paramagnetism in the temperature range of 5 to 300 K. This evidences a robust room-temperature-ferromagnetism (RTFM) in these NPs. The RTFM of our samples is attributed to the presence of oxygen vacancies in our samples.

Keywords: DMS, nanoparticles, defect states, magnetic property, X-ray diffraction.

INTRODUCTION

Over the last decade, DMS is a main ingredient of research due to its potential applications in spintronic. A number of nonmagnetic metal oxides such as ZnO, SnO_2, TiO_2, and In_2O_3, exhibit ferromagnetic behavior when doped with suitable magnetic transition metals (TM). Beside magnetically doped metal oxides, a number of undoped metallic oxide thin films and NPs also show ferromagnetism. The origin of the ferromagnetism in these doped and undoped metal oxides still remains controversial. Anna *et al*. [1] have obtained Fe doped ZnO nanofibers through electrospinning and observed room temperature ferromagnetism. These authors have shown that low temperature ferromagnetism in their samples arises due to Fe atom substituting Zn in the ZnO lattice. This study suggests that the ferromagnetism is either due to defect (oxygen vacancy) mediated Fe-Fe exchange interaction or is related to iron-rich precipitates.

Recently, In_2O_3 NPs of different morphologies like nanowires, nanocrystal chains, nanorods, nanobelts, nanotowers, hollow spheres, nanotubes, microarrows have been successfully synthesized by different methods. In_2O_3 is quite complicated and different from other DMS as it has higher solubility limit for TM ions. Many TM ions have been employed as dopants in In_2O_3 in order to get ferromagnetisms. For example, He *et al*. [2,3] have carried out systematic studies on ferromagnetism of co-doped (Fe, Cu) and Fe doped In_2O_3 nanostructures. On the other hand, Be´rardan *et al*. synthesized Fe doped In_2O_3 [3] by same method and proposed that it showed ferromagnetic properties. According to earlier theoretical studies only oxygen-rich surfaces of oxides can have magnetization which inspires many researchers to study the origin of the magnetism in oxygen-depleted oxides like In_2O_3. Although, room temperature ferromagnetism is observed in transition metal doped Indium oxide, the origin of ferromagnetism is still unclear. Therefore, we decided to work on Fe doped In_2O_3 NPs to explain the possible origin of ferromagnetism.

METHOD AND MATERIALS

The wet chemical method is used to synthesize Fe doped In_2O_3 nanoparticles [4]. Starting precursors of indium chloride (analytical grad, Aldrich) and iron(III) chloride hexahydrate (analytical grad, Aldrich) were dispersed in double-distilled water (solution-I) followed by drop-wise addition of i-PrOH in solution-I under vigorous stirring at 60°C. Finally, metal oxide precipitate was recovered by hydrolysis through weak ammonia solution. The as-received powder was washed several times with absolute ethanol and dried overnight at ~50°C. All samples were annealed in a tubular furnace at 400°C. The phase and crystal structure of the samples were examined by XRD using Cu Kα radiation from 2θ = 10 to 70°. Transmission

*Address correspondence to this author at the Department of Physics, Federal Urdu University of Arts, Science and Technology Karachi Pakistan; E-mail: rizwan@fuuast.edu.pk

ISSN: 1814-8085 / E-ISSN: 1927-5129/17

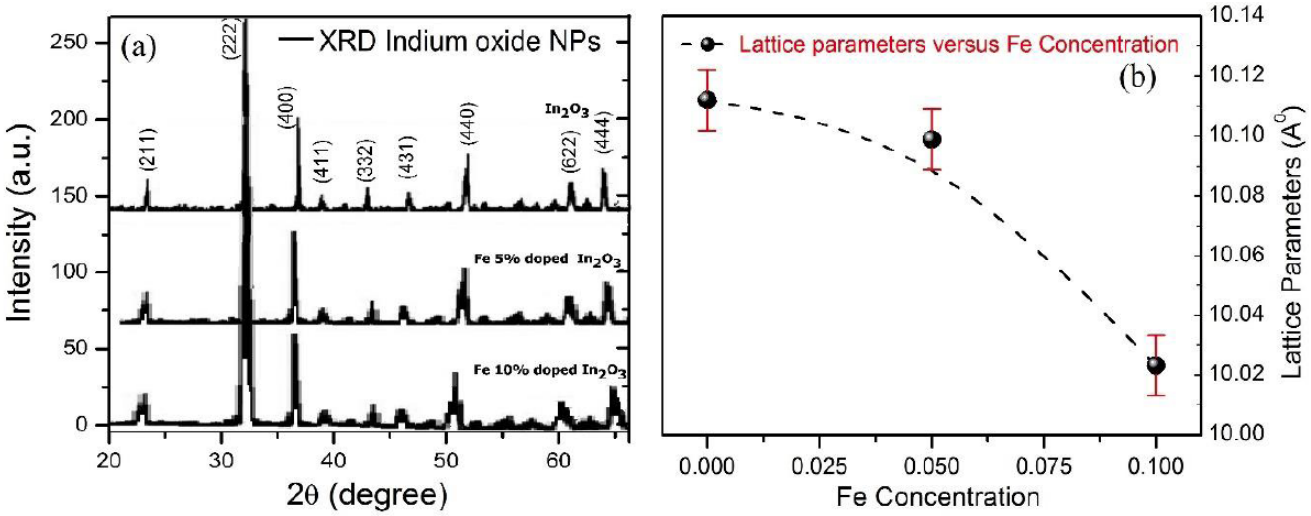

Figure 1: (**a**) X-ray diffraction spectra; (**b**) variation of lattice constant versus Fe concentration.

electron microscope (TEM) and high-resolution TEM (HRTEM) are used to parameterize the particle size and examine the presence of secondary phases. Field and temperature-dependent magnetic behaviour of all nanoparticles was determined by a physical property measurement system (PPMS, Quantum Design, U.S.A) equipped with 1T magnet.

RESULTS AND DISCUSION

Figure **1** shows x-ray diffraction pattern of the sample. Comparing with the data files joint committee on powder diffraction standards (JCPDS No. 6-0416), it was found that resulting peaks are in fair agreement with the standard pattern. The peak positions are marked by their respective planes indices. The most intense peak or preffered peak of our particle is at plane (222). No secondary phase of iron oxides are observed within the detection limit (1%) of the XRD. The shifting of (222) peak towards higher 2θ values indicates successful incorporation of Fe in to indium oxide lattice. This peak shifts is due to smaller Fe^{3+} ions (ionic radius R_{Fe}^{3+}= 0.645 Å) replacing larger In^{3+} ions (ionoic radius R_{In}^{3+}=0.80 Å) in In_2O_3 lattice. The average crystallite size is determined from the peak widths using Scherer's formula equ. 1.

$$D_v = k\lambda / \beta_D \cos\theta \quad (1)$$

where D_v is the particle size, θ is the Bragg angle, λ is the wavelength of x-ray, K is a constant which depends upon the particle shape and β_D is the peak broadening (i.e., full-width at half-maxima measured in radian). Typically, values of K lie between 0.85 and 0.99. For our instrument λ=1.54 Å and K= 0.91.

Table 1: Compression of Particle Sizes Estimated from Different Methods.

Size (Scherrer's)	Size (W-H Plot)	Strain
21 nm	18 nm	-9.91742
23 nm	22 nm	-8.89366
27 nm	24 nm	-6.6716

Concentration analysis			
Sample	**Elements**	**Concentration (χ)×10^{-3}**	**Oxygen vacancies (O/In)**
Undoped In_2O_3	In O Fe	57.02 42.98 -	0.75377
Fe 5% Doped In_2O_3	In O Fe	56.79 38.34 4.87	0.67511
Fe 10% Doped In_2O_3	In O Fe	54.28 35.96 9.76	0.66249

In order to get a better estimate of crystallite size and strain, the Williamson adopted a method. If the the size and strain are Lorentz profile, the induced strain ε and peak broadening β_S are related by

$$\beta_S = 4\varepsilon \tan\theta \quad (2)$$

The total broadening β_t will be the sum of β_D (Scherer's equation) and β_S (as estimated from induced strain broadening eq (2)):

$$\beta_t = \beta_S + \beta_D \quad (3)$$

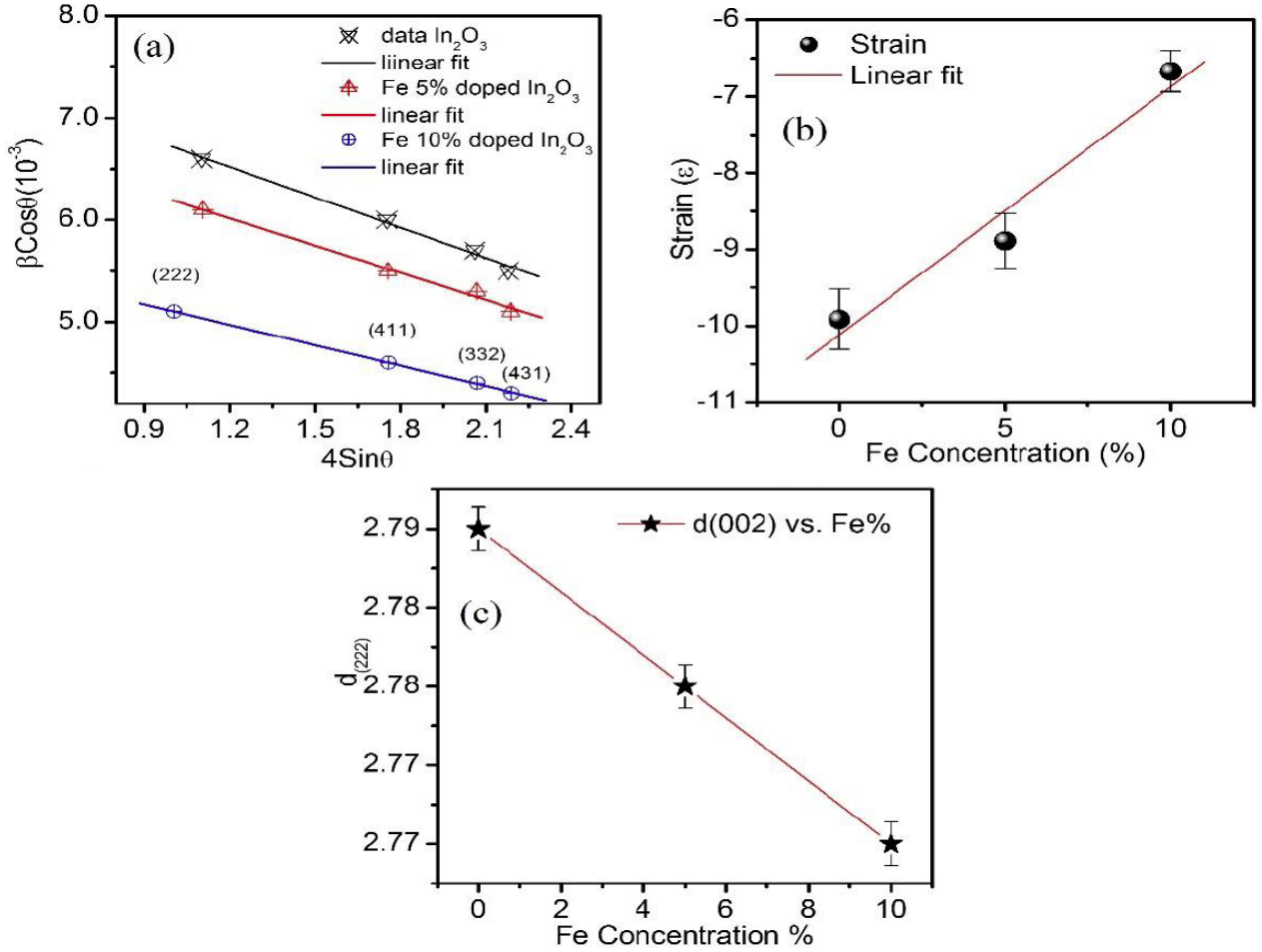

Figure 2: (**a**) Williamson Hall plot for all samples; (**b**) Plot of strain versus Fe concentration; (**c**) Plot of interplanner spacing; (**d**) versus Fe concentration.

$$\beta_t \cos\theta = 4\varepsilon \sin\theta + \frac{k\lambda}{D} \quad (4)$$

Equation (4) is like an line equation of slope intercept form so Williamson deduce that by plotting $\beta_t \cos\theta$ against $4\sin\theta$ a straight line is obtained whose slope will be equal to Strain and intercept will be equal to $\frac{k\lambda}{D}$ .We have plotted the Williamson Hall (WH) plots for (222), (411), (332) and (431) diffracted XRD peaks of undoped, 5% and 10% Fe doped In_2O_3 nanoparticles in Figure **2a**. After plotting the WH plot we calculate the size and strain from the linear fit to the data. Table **1** gives a comparasion of the particle size as estimated by Scherer formula and WH plot. Clearly, the particle size by Scherer's formula is greater than the one estimated by WH plot. This is due to the fact that Scherer`s equation does not take into account of the strain which was induced by Fe doping. Thus, WH plot give a better estimate of the particle size than Scherer`s formula.

The negative value of strain (see Figure **2b**) for the In_2O_3 nanoparticles indicates compressional strain in the lattice. In a next step, we plot interplanner spacing ($d_{(002)}$) over Fe concentration followed by Vegard's linear fit in Figure **2c**. The interplaner spacing is found to be decreaseing with increasing Fe concentration.

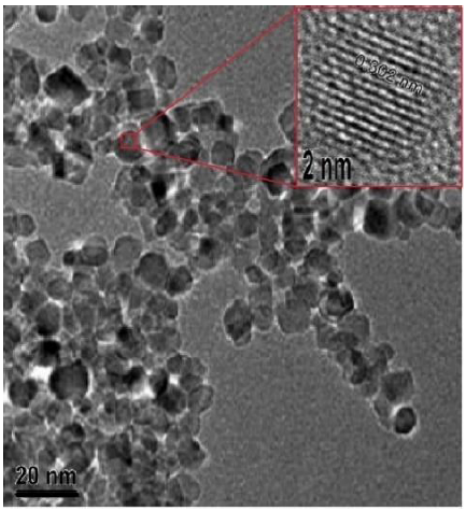

Figure 3: Transmission electron micrograph of In_2O_3 nanoparticle.

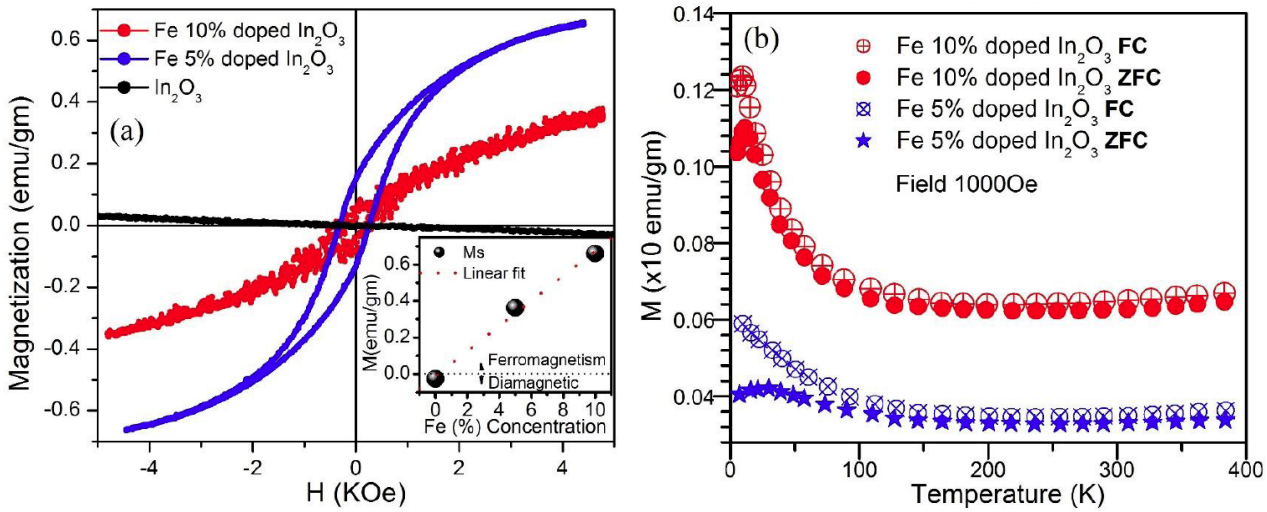

Figure 4: (**a**) MH loops of all samples (inset) Plot of magnetization versus Fe concentration; (**b**) FC and ZFC curves of ferromagnetic nanoparticles at 1000Oe.

The structural characterization was also carried out by TEM and HRTEM. Figure **3** shows a TEM image of pure In_2O_3 nanoparticles. The average size of the particle determined by TEM is 18 nm which is in good agreement with WH Plot data. The HRTEM image of the nanoparticles also shows well-defined lattice planes, indicating the single crystalline nature of our nanoparticles. The interplanar spacing is extracted to be 3.02 Å which corresponds to the (222) plane of the cubic In_2O_3. The EDX analysis was carried out (not shown here) to determine the chemical composition of our NPs. For pure sample the ratio between O ions and In ions is found to be standard 3:2 (1.50). However, this ratio is less than the standard ration (3:2) for doped samples (given in table 1). This implies that there is plenty of O vacancies (V_o) are present in our samples.

In order to see the effect of V_o on the magnetic response of oue samples detailed magnetic characterizations of our samples were carried out using using a physical property measurement system equipped with 1T magnet. The magnetic properties of the nanoparticles are generally studied by observing the response of the material for a given applied magnetic field. For the present samples the magnetic data are recorded in the temperature range 4 – 300 K. Figure **4a** shows DC magnetization curve for undoped, 5% and 10% Fe doped In_2O_3 nanoparticles at 300 K temperature. It can be seen that the undoped sample exhibit nonmagnetic behavior while the doped samples show hysteric behavior which indicates ferromagnetic order in the sample. It is obvious from Figure **4a** that the saturation magnetization (M_s) increases from 0.34 emu/mg to 0.65 emu/mg when Fe doping concentration goes 5% to 10%.

For a better understanding of the origin of room temperature ferromagnetism in our Fe doped In_2O_3 nanoparticles we measure the dc magnetization of the sample after cooling the sample from 325 K to 5 K either in zero field cooled (ZFC) or in 1 kOe (FC). For both cases the data are recorded during warming of the sample from 5 K to 325 K in a small static field. As there is a clear divergence present between ZFC and FC curves over the long range temperature from 5 K to 300 K and no indication of transition from ferromagnetic to paramagnetic behavior could be observed [5]. The origin of ferromagnetism in our Fe doped In_2O_3 nanoparticles is explained as follows: doped samples contain significant number of oxygen vacancies (V_o) as confirmed by strcutral chrctrization. The Fe dopant (Fe^{+3} or Fe^{+2}) as local moment interact with the delocalize states of V_o and form a bound magntic polaron [6]. A bound magnetic polaron is regarded as a $In^{3+}(\uparrow)$-$V_o(\downarrow)$-$Fe^3(\uparrow)$ or $Fe^3(\uparrow)$-$V_o(\downarrow)$-$Fe^3(\uparrow)$ complex where a net aligned spin is present. This leads to long range ferromagnetic order after overlaping of nearby magnetic polarons. Hence, this might be one of the possible origin of ferromagnetism in our Fe doped In_2O_3 nanoparticles

CONCLUSION

Different samples of pure and Fe doped Indium oxide (In_2O_3) nanoparticles were prepared and characterized. All undoped and Fe doped indium oxide samples were crystallized in cubic bixbyite structure. TEM and HRTEM images show that un-doped indium oxide nanoparticles have almost spherical shape and narrow size distribution. Magnetic measurements show that saturation magnetization increases with increasing

Fe concentration. FC and ZFC measurements show that maximum magnetization observed near 5K for which it found to be decreased with increasing temperature. The origin of observed ferromagnetism has successfully explainedby the bound magnetic polarons.

ACKNOWLEDGEMENTS

The authors gratefully acknowledge the financial support by Federal Urdu University of Arts, Science & Technology through mini-project grant 2016-17.

REFERENCES

[1] Baranowska-Korczyc A, Reszka A, Sobczak K, Sikora B, Dziawa P, Aleszkiewicz M, Kłopotowski L, Paszkowicz W, Dłużewski P, Kowalski BJ, Kowalewski TA. Magnetic Fe doped ZnO nanofibers obtained by electrospinning. Journal of Sol-Gel Science and Technology 2012; 61(3): 494-500. https://doi.org/10.1007/s10971-011-2650-1

[2] He J, Xu S, Yoo YK, Xue Q, Lee HC, Cheng S, Xiang XD, Dionne GF, Takeuchi I. Room temperature ferromagnetic n-type semiconductor in (In 1− x Fe x)2O3−σ. Applied Physics Letters 2005; 86(5): 052503. https://doi.org/10.1063/1.1851618

[3] Bérardan D, Guilmeau E, Pelloquin D. Intrinsic magnetic properties of In2O3 and transition metal-doped-In2O3. Journal of Magnetism and Magnetic Materials 2008; 320(6): 983-9. https://doi.org/10.1016/j.jmmm.2007.10.002

[4] Qaseem S, Ali SR, Naeem M, Rizvi S. Size induced ferromagnetism in pristine indium oxide nanoparticles. Applied Surface Science 2015; 331: 87-91. https://doi.org/10.1016/j.apsusc.2015.01.012

[5] Qaseem S, Naeem M, Ali SR, Maqbool M, Ali SI. Tunable High-T_C ferromagnetism in Sn^{4+}-doped $(InFe_{0.04})_2O_3$ nanoparticles: a vital role of electron doping. Materials Technology 2017; 32: 327-333. https://doi.org/10.1080/10667857.2016.1217117

[6] Coey JM, Venkatesan M, Fitzgerald CB. Donor impurity band exchange in dilute ferromagnetic oxides. Nature Materials 2005; 4(2): 173-9. https://doi.org/10.1038/nmat1310

Received on 01-06-2017 Accepted on 15-06-2017 Published on 21-06-2017

https://doi.org/10.6000/1927-5129.2017.13.61